MICROBUNCHING INSTABILITY AS A CAUSTIC PHENOMENON

T. K. Charles*, D. M. Paganin, School of Physics and Astronomy, Monash University, Australia

M. J. Boland[1], R. T. Dowd, Australian Synchrotron, Clayton, Australia

[1]also at School of Physics, University of Melbourne, 3010, Victoria, Australia

Abstract

Microbunching instability if left alone, threatens to degrade the beam quality of high brightness electron beams in Free Electron Lasers. Recently, caustic formation in electron trajectories was identified as a mechanism describing current modulations in accelerated particle beams. Here we consider CSR-induced microbunching as a caustic phenomenon. This analysis reports on the influence of longitudinal dispersion, R_{56}, on the microbunching process, as well as elucidating the influence of the second and third order longitudinal dispersion values, T_{566} and U_{5666}.

INTRODUCTION

Within an FEL linac bunch compressor, small initial density or energy modulations can be amplified through the longitudinal dispersion (R_{56}) of the compressor and through the influence of Coherent Synchrotron Radiation (CSR) produced by short bunches traversing a bend. If left unattended, this microbunching instability can grow, leading to beam quality degradation and compromised FEL performance. Much research effort has been invested into microbunching including extensive theoretical [1–4] and experimental investigation [5–8].

Many techniques have been theorized and implemented that successfully limit the evolution of microbunching instability [9–12]. In the work presented here, we view the microbunching as a caustic phenomenon, which gives us insight into the factors that influence the microbunching severity, some of which are often not considered as integral to the microbunching process.

In a recent paper, caustic formation in particle trajectories was identified as being the fundamental mechanism that drives intense current modulations in dispersive regions [13]. Caustics are the regions of intense current (or light) introduced by a form of "natural focusing" whereby adjacent particle trajectories (or rays of light) to coalesce [15, 16]. Common examples of caustics in optics are the bright lines seen in a well-lit coffee cup, or the moving networks of bright light that can appear on the bottom of swimming pools. The recent paper [17] considered caustic applications to accelerator physics, which has been directly associated with current horns that appear in strong bunch compression [13]. In this paper we realize the application of caustic theory to microbunching instability. It can be noted that a similar approach could be applied to the desirable microbunching that occurs in the undulator section further upstream in an FEL facility.

MICROBUNCHING CAUSTICS

At the end of a dispersive region, the parametric form for the set of caustic points ($\tilde{z}, \tilde{R_{56}}$), parameterized by the initial longitudinal position z_i is, (see Eq. (8) in [13]),

$$\tilde{z}(z_i) = z_i - \frac{\delta(z_i)}{\delta'(z_i)} - T_{566}\delta^2(z_i) - 2U_{5666}\delta^3(z_i) \quad (1a)$$

$$\tilde{R_{56}}(z_i) = \frac{-1}{\delta'(z_i)} - 2T_{566}\delta(z_i) - 3U_{5666}\delta^2(z_i), \quad (1b)$$

where $\delta(z_i)$ is the shape of the initial longitudinal phase space distribution or chirp, the dash denotes a derivative with respect to z_i and R_{56}, T_{566}, and U_{5666} are the first-, second-, and third-order longitudinal dispersion values respectively.

The longitudinal phase space shape, $\delta(z_i)$, is often described by a high-order polynomial. For the case of studying microbunching, we will instead introduce a sinusoidal energy modulation that could be imparted on to the beam through longitudinal space charge forces, shot noise or noise in the photo-gun laser for example. That is, the longitudinal phase space distribution will be described as,

$$\delta(z_i) = h_1 z_i + a\sin(kz_i) \quad (2)$$

where a and k are the initial energy modulation amplitude and wave number respectively, and h_1 is the first-order energy chirp.

Incorporating Eq. (2) into Eq. (1) we can determine the caustic points, which represent the longitudinal positions of the current spikes for various R_{56} values. The result is shown in Fig. 1, for the given initial values of $a = 0.01\%$, and $k = 2.5 \times 10^{-5}$ m^{-1}. In the case detailed below, an R_{56} value of -12.4 mm indicates maximum compression, and $R_{56} < $ -12.4 mm results in an over-compressed bunch.

The current profile at any value of R_{56} can be calculated using the analytical expressions derived in reference [13] and demonstrated in [14]. Using this expression, the current profiles have been evaluated for a set of R_{56} values, marked as abscissae in Fig. 2. The results are shown in Fig. 3.

The initial modulation greatly influences the caustic curves. Figure 4 is illustrative of this, where a is doubled from the red to the orange curves. This change in the initial modulation amplitude shifts the longitudinal position of the current peaks (caustics) for any chosen R_{56} value.

INFLUENCE OF R_{56}, T_{566} AND U_{5666}

From Fig. 1 it is clear that R_{56} can have a dramatic effect on the microbunching development. This is also known from the theoretical work presented in references [2,3,18,19]. The
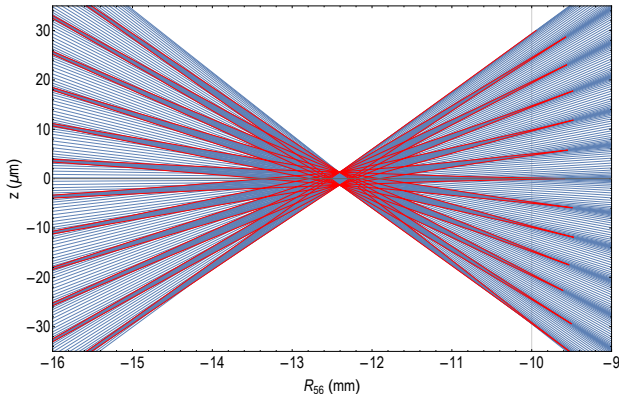
05 Beam Dynamics and Electromagnetic Fields

D05 Coherent and Incoherent Instabilities - Theory, Simulations, Code Developments

Figure 1: Caustic expression [Eq. (1)] shown in red overlaid on blue electron trajectories, showing where in z current spikes can be anticipated for a given R_{56} value, for a 4 dipole chicane where $T_{566} = U_{5666} = 0$.
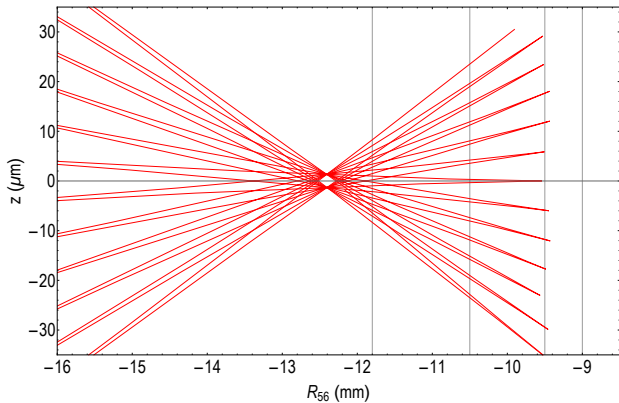

Figure 2: Caustic expression [Eq. (1)] showing values of R_{56} corresponding to the current profiles shown in Fig. 3.
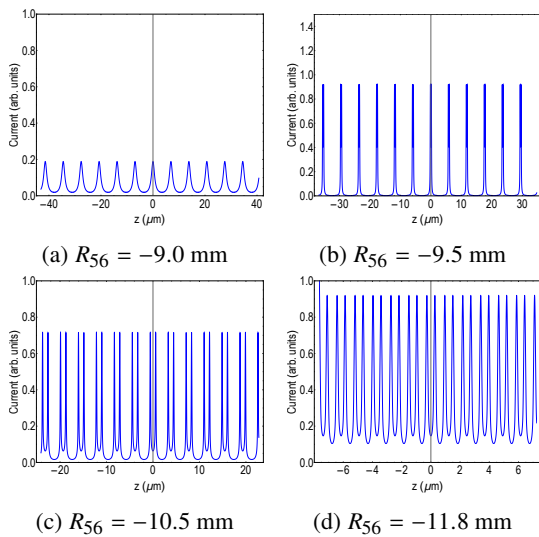

(a) $R_{56} = -9.0$ mm   (b) $R_{56} = -9.5$ mm

(c) $R_{56} = -10.5$ mm   (d) $R_{56} = -11.8$ mm

Figure 3: Current profiles bifurcation of current peaks for various R_{56} values shown in Fig. 2.

instability is also sensitive to the choice of the second- and third-order longitudinal dispersion values, T_{566} and U_{5666}.
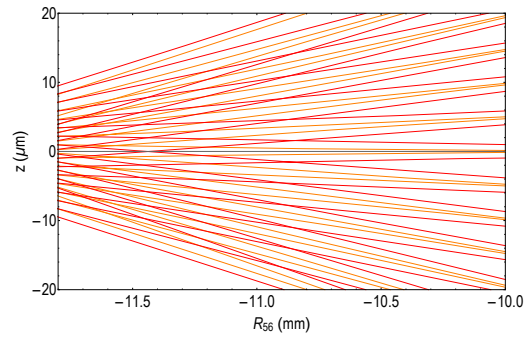
Figure 4: Caustic lines where a is doubled from $a = 0.01\%$ (red) to $a = 0.02\%$ (orange).

The caustic points [calculated with Eq. (1), shown in Fig. 1] are shown again in Figures 5 and 6 with altered values of T_{566} and U_{5666} respectively. The orange curves in both Figures 5 and Fig. 6, are the same as Fig. 2 where $T_{566} = U_{5666} = 0$. The red curve in Fig. 5 was calculated with $T_{566} = -30$ mm. The red curve in Fig. 6 was calculated with $U_{5666} = -2$m.

T_{566} has the effect of folding the caustic curves over themselves, (to give a "caustics of caustics") where caustic points that were originally at large positive values of z are shifted to lower values. If T_{566} were instead positive, this shift in z would move in the opposite direction. As for U_{5666}, by increase $|U_{5666}|$ the caustic points shift to the right in Fig. 6.
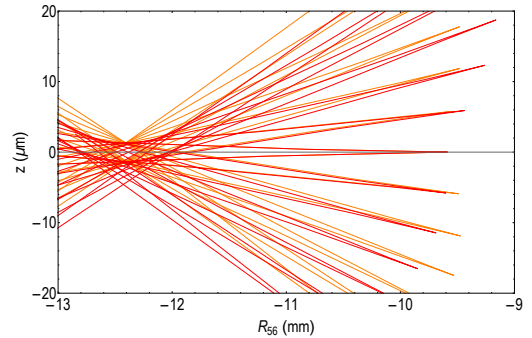

Figure 5: Caustic expression indicating longitudinal positions of current spikes for $T_{566} = 0$ (orange) and $T_{566} = -30$ mm (red).

GAIN CURVE

The Gain function for an initial modulation wavenumber, k_0, is commonly defined as,

$$G(k_0) = \frac{|b_f(k_f)|}{|b_0(k_0)|} \quad (3)$$

where $b_f(k_f)$ and $b_0(k_0)$ are the final and initial bunching factors where k_f is the wavenumber after compression and therefore modified by the compression factor from the initial wavenumber, k_0. The bunching factor is calculated by,
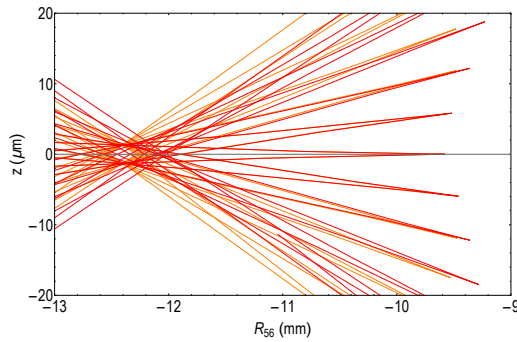
$$b(k) = \frac{1}{Nec} \int I(x)e^{-ikz} dz. \quad (4)$$

Figure 6: Caustic expression indicating longitudinal positions of current spikes for $U_{5666} = 0$ (orange) and $U_{5666} = -2$m (red).

Code was written to propagate 10^5 Gaussian distributed particles through a dispersive region after an initial sinusoidal energy modulation was imprinted along the bunch.

For an R_{56} of -10 mm, the resulting gain curve is shown in Fig. 7. Visible in Fig. 7 is are series of small peaks before the broad large peak of the gain curve. This behavior is evident in few a publications such as references [5, 9, 20]. An explanation of how and why the gain curve drops close zero is provided below.
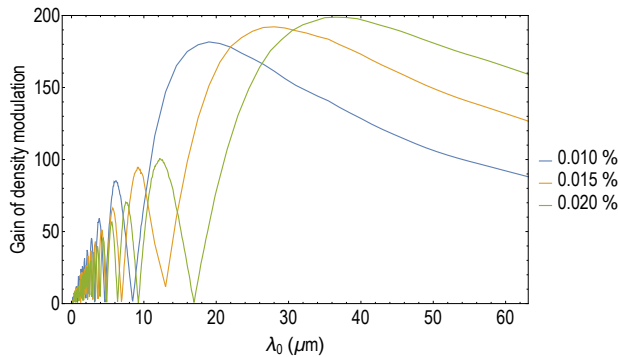

Figure 7: Gain curve as defined by Eq. (3).

Gain Curve Oscillatory Behavior

At low initial modulation wavelengths, the gain curve drops to zero, however this is misleading as the bunching does not dissipate at these wavelengths. In fact, the opposite in true. The caustic nature of the microbunching can lead to bifurcation of the current peaks as shown in Fig. 3. Where the gain curve drops to zero, (*e.g.* $\lambda_0 = 8.3\mu$m of Fig. 7 blue curve), corresponds to where the bifurcated peaks are separated by $\lambda_0/2$. Therefore when Eq. (4) is used to calculate the bunching factor at k_f, the resulting calculation yields zero as particles now appear evenly in both the peaks and troughs of the sampling sinusoidal signal, $e^{-ik_k z_k}$.

Figures 8 and 9 demonstrate the how the caustic expression changes for different values of λ_0 and the associated current peaks. The values of λ_0 chosen for Fig. 8 and Fig. 9 are 8.3 μm and 20 μm respectively. These values correspond to where the gain curve is low (close to zero) and

high (see blue curve of Fig. 7). As can be seen in Fig. 9, for $\lambda_0 = 8.3\mu$m the peaks have split such that there is an equal distance between all of the split peaks.
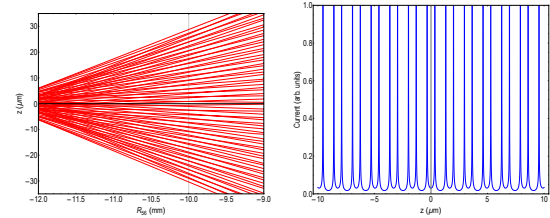

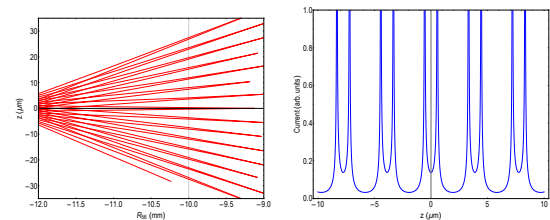Figure 8: Caustic expression and current profile corresponding to $R_{56} = -10$mm, for $\lambda_0 = 8.3\mu$m.

Figure 9: Caustic expression and current profile corresponding to $R_{56} = -10$mm, for $\lambda_0 = 20\mu$m.

CONCLUSION

In this work, microbunching instability was considered as a caustic phenomenon. This approach provides insight into the bifurcation of current peaks that can result in the misleading result of the gain curve going to zero at low values of the initial modulation wavelength. This suggests a new formulation of the gain curve could be needed to accurately describe the impact of microbunching for low values of the initial modulation wavelength, λ_0. In addition, the influence of T_{566} and U_{5666} were investigated showing that the development of the microbunching is heavily dependent upon these two parameters.

REFERENCES

[1] E. Saldin, E. Schneidmiller, and M. Yurkov, "On the coherent radiation of an electron bunch moving in an arc of a circle," Nucl. Instr. Meth. Phys. Res. A, vol. 398, pp. 373–394, 1997.

[2] Z. Huang and K. J. Kim, "Formulas for coherent synchrotron radiation microbunching in a bunch compressor chicane," Phys. Rev. ST Accel. Beams, vol. 5, p. 074401, 2002.

[3] S. Heifets, G. Stupakov, and S. Krinsky, "Coherent synchrotron radiation instability in a bunch compressor," Phys. Rev. ST Accel. Beams, vol. 5, p. 064401, 2002.

[4] M. Venturini, "Microbunching instability in single-pass systems using a direct two-dimensional Vlasov solver," Phys. Rev. ST Accel. Beams, vol. 10, p. 104401, 2007.

[5] D. Ratner, C. Behrens, Y. Ding, Z. Huang, A. Marinelli, T. Maxwell, and F. Zhou, "Time-resolved imaging of the microbunching instability and energy spread at the Linac Coherent Light Source," Phys. Rev. ST Accel. Beams, vol. 18, p. 030704, 2015.

[6] H. Loos et al., "Observation of coherent optical transition radiation in the LCLS linac," *Proc. FEL08*, Gyeongju, Korea, Aug. 2008, paper THBAU01, pp. 485–489.

[7] A. H. Lumpkin, N. S. Sereno, W. J. Berg, M. Borland, Y. Li, and S. J. Pasky, "Characterization and mitigation of coherent-optical-transition-radiation signals from a compressed electron beam," *Phys. Rev. ST Accel. Beams*, vol. 12, p. 080702, 2009.

[8] A. H. Lumpkin, R. J. Dejus, and N. S. Sereno, "Coherent optical transition radiation and self-amplified spontaneous emission generated by chicane-compressed electron beams," *Phys. Rev. ST Accel. Beams*, vol. 12, p. 040704, 2009.

[9] Z. Huang, M. Borland, P. Emma, J. Wu, C. Limborg, G. Stupakov, and J. Welch, "Suppression of microbunching instability in the linac coherent light source," *Phys. Rev. ST Accel. Beams*, vol. 7, p. 074401, 2004.

[10] J. Qiang, C. E. Mitchell, and M. Venturini, "Suppression of microbunching instability using bending magnets in free-electron-laser linacs," *Phys. Rev. Lett.*, vol. 111, p. 054801, 2013.

[11] S. Di Mitri and S. Spampinati, "Microbunching instability suppression via electron-magnetic-phase mixing," *Phys. Rev. Lett.*, vol. 112, p. 134802, 2014.

[12] S. Di Mitri, M. Cornacchia, S. Spampinati, and S. Milton, "Suppression of microbunching instability with magnetic bunch length compression in a linac-based free electron laser," *Phys. Rev. ST Accel. Beams*, vol. 13, p. 010702, 2010.

[13] T. K. Charles, D. M. Paganin, and R. T. Dowd, "Caustic-based approach to understanding bunching dynamics and current spike formation in particle bunches," *Phys. Rev. AB*, vol. 19, p. 104402, 2016.

[14] T. K. Charles et al., "Beam by Design: Current Pulse Shaping Through Longitudinal Dispersion Control", MOPIK055, *These Proceedings*, IPAC'17, Copenhagen, Denmark (2017).

[15] M. V. Berry and C. Upstill, "Catastrophe Optics: Morphologies of Caustics and Their Diffraction Patterns," *Prog. Opt.*, vol. 18, pp. 257–346, 1980.

[16] J. F. Nye, "Natural Focusing and Fine Structure of Light Caustics and Wave Dislocations", Philadelphia, USA: Taylor & Francis, 1999.

[17] T. K. Charles, D. M. Paganin, A. Latina, M. J. Boland, and R. T. Dowd, "Current-horn suppression for reduced coherent-synchrotron-radiation- induced emittance growth in strong bunch compression," *Phys. Rev. Accel. Beams*, vol. 030705, 2017.

[18] E. L. Saldin, E. A. Schneidmiller, and M. V. Yurkov, "Klystron instability of a relativistic electron beam in a bunch compressor," *Nucl. Instr. Meth. Phys. Res. A*, vol. 490, pp. 1–8, 2002.

[19] Z. Huang, J. Wu, and T. Shaftan, "Microbunching Instability due to Bunch Compression," *ICFA Beam Dyn. Newsl.*, vol. 38, pp. 37–50, 2005.

[20] M. Venturini, "The Microbunching Instability and LCLS-II Lattice Design," *Proc. FEL2015*, Daejeon, Korea, Aug. 2015, paper TUC01, pp. 308–316.